LCLC Resonant Converter as Maximum Power Point Tracker in PV Systems

Alfonso Conesa, Guillermo Velasco, Herminio Martínez and Manuel Román
Technical University of Catalonia (EUETIB / UPC)
C/ Comte d'Urgell, 187. E–08036
Barcelona, SPAIN
E-Mail: alfonso.conesa@upc.edu

Acknowledgements

This work has been partially funded by project DPI-2006–15627–C03–01 from the Spanish MCYT and EU FEDER funds.

Keywords

Resonant converters, Maximum power point tracker (MPPT), Photovoltaic (PV), DC power supply, Modeling.

Abstract

This paper presents the analysis and implementation of an LCLC resonant converter working as maximum power point tracker (MPPT) in a PV system. This converter must guarantee a constant DC output voltage and must vary its effective input resistance in order to extract the maximum power of the PV generator. Preliminary analysis concludes that not all resonant load topologies can achieve the design conditions for a MPPT. Only the LCLC and LLC converter are suitable for this purpose.

Introduction

Resonant load converters are a kind of converters widely used in DC-DC applications. However, their use as intermediate stage between the PV generator and the inverter in PV systems is not in excess considered in the bibliography ([1], [2]). There are different resonant load topologies, but not all these are suitable to guarantee a constant DC output voltage and vary the effective input resistance. Thus, the analysis begins with selecting a proper resonant load topology

It is assumed that the MPP voltage of the PV generator has a small variation for a large range of irradiance levels. This voltage is a value close to the open circuit voltage [3]. The variations of the MPP vary the maximum power available on the PV generator, being the current on the MPP the magnitude with main variation. Figure 1 shows the I-V characteristic of a PV generator for different irradiance values (G_1 and G_2).

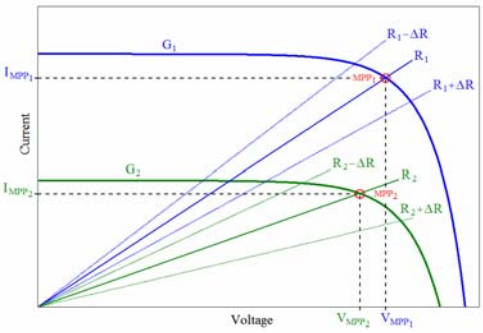

Fig. 1: I-V characteristic of a PV generator depending on the irradiance (G_1 and G_2)

Thus, it is necessary that the DC-DC converter allows variations of its effective input resistance as is presented in figure 2.

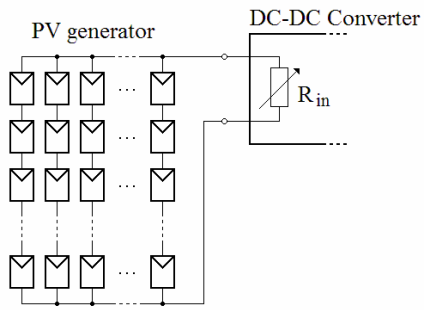

Fig. 2: DC-DC converter input resistance desired behavior

The variation range of the effective input resistance (minimum and maximum value) must be known to select the working point of the converter. This depends on the irradiance values and the PV modules association in the PV generator. The variation range of the effective resistance has important influence on the design specifications of the converter. Depending on this range will affect the interval of variation of switching frequency and the values of resonant components.

In the analysis for selecting the working point of the converter and values of the components is where we found the greatest difficulty, due to the large number of interdependent constants involved in this kind of converters.

Study of the different resonant load topologies

The method of the first harmonic approximation is used to analyze different topologies of resonant converters as possible structures for use as MPPT. This method of analysis is applied to resonant converters because it greatly simplifies the task of analysis. The error obtained in the approximation is acceptable for most of the analysis if the switching frequency of the converter is close to the resonance frequency of the resonant tank [4].

The analysis considers the four basics topologies of resonant converters: the Parallel Resonant Converter (PRC), the LLC or Series Resonant Converter (SRC), the LCC or Series Parallel Resonant Converter (SPRC) and the LCLC. The analysis is focused to analyze the output voltage and input effective resistance for each converter with respect to the load and switching frequency values.

These converters are frequency variation controlled. Thus, it is necessary to select a range of frequency variations according to the desired range of input resistance variation. Because the input voltage is assumed as a constant value, by selecting the proper frequency it is possible to vary the input current of the converter and, consequently, vary the operating point of the PV generator. Figure 3 shows the ideal behavior of the output voltage and input resistance which the resonant converter must guarantee with respect to the switching frequency when the PV generator input power varies. Figure 3 presents a negative slope of variation of the input power (therefore a positive slope on input resistance) increasing the switching frequency. However, depending on the converter behavior (input impedance and transfer function), another alternative option is that when increasing the switching frequency the slopes presented in figure 3 (R_{IN} and P) can have an opposite sign. These two magnitudes are related according to equation (1) if we consider the efficiency (η) and the output voltage of the converters as constant values.

$$P_{Out} = \eta P_{In} \qquad R_L = \frac{1}{P_{In}} \cdot \frac{{V_{Out}}^2}{\eta} \tag{1}$$

Two additional considerations were taken into account to decide which resonant topology is the most appropriate. One is that the value of reactive power that appears in the resonant tank should be as small as possible, in order to reduce conduction losses in the switches. The second one is that the impedance of the tank should be inductive, in order to reduce switching losses.

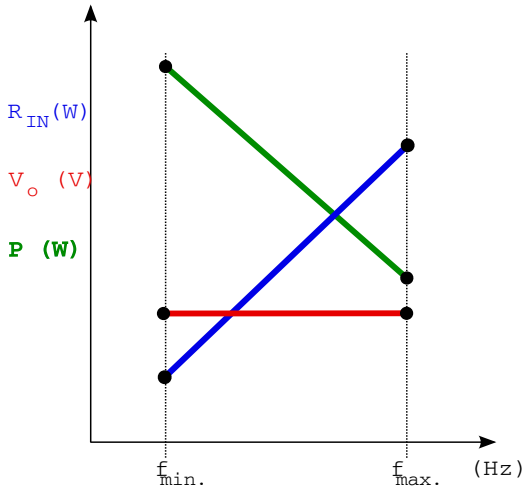

Fig. 3: Ideal behavior of the output voltage, input resistance and input power in the resonant converter with respect to the switching frequency

Figure 4 shows for the different resonant topologies in study the normalized output voltage (red color), the resonant tank impedance (black color), the converter input resistance (blue color) and the output effective resistance (magenta color) with respect to the normalized frequency. The normalized output voltage is defined as $n \cdot V_o / V_{gen}$, being n the transformer turn ratio, V_o the output voltage of the converter and V_{gen} the input voltage of the converter. The normalized frequency is the switching frequency with respect to the resonant frequency (f_s/f_o).

Figure 4, for the PRC, shows that if the switching frequency is below resonance the output voltage is a constant value and can vary the converter input resistance (Region of Interest ROI_A). These are the desired design conditions, but the behavior of the resonant tank becomes capacitive. Furthermore, this range of frequencies is far enough from the resonant value, being necessary a bulky resonant inductor and capacitor. Finally, these results of the first harmonic analysis can contain unacceptable errors because this switching frequency range is far away from the resonance frequency of the resonant tank. All these considerations lead to not recommend the parallel converter as a possible MPPT.

Figure 4 for the LCC or SPRC correspond to a capacitor relation $k_C=C_p/C_s=0.1$. This is the best case found with respect to $k_C=1$ or $k_C=10$. If the switching frequency is close to resonant frequency (ROI_B) may be found a flat response on the output voltage and an important variation of the input resistance. But it presents a non desired capacitive behavior, and lead to not recommend the LCC converter.

Figure 4 for the LLC corresponds to a inductor relation $k_L=L_p/L_s=10$. This is the best case found with respect to $k_L=0.1$ or $k_L=1$. If the switching frequency is close to the resonant frequency (ROI_C) there is a small variation on the output voltage and a large variation on the input resistance. The tank impedance keeps close to the input resistance and presents inductive behavior. Therefore the LLC can be a good candidate to MPPT.

Finally in figure 4, the LCLC corresponds to the case $k_L=1$ and $k_C=0.5$. This figure shows the influence of the two resonances in the converter due to the series impedance and parallel impedance of the topology. Between the two resonant frequencies of the converter (ROI_D) there is a range of frequencies with almost constant output voltage and large input resistance variation. Furthermore the

impedance of the resonant tank is proportional and close to the input resistance, and presents inductive behavior. All these considerations lead to recommend the LCLC converter as a possible MPPT.

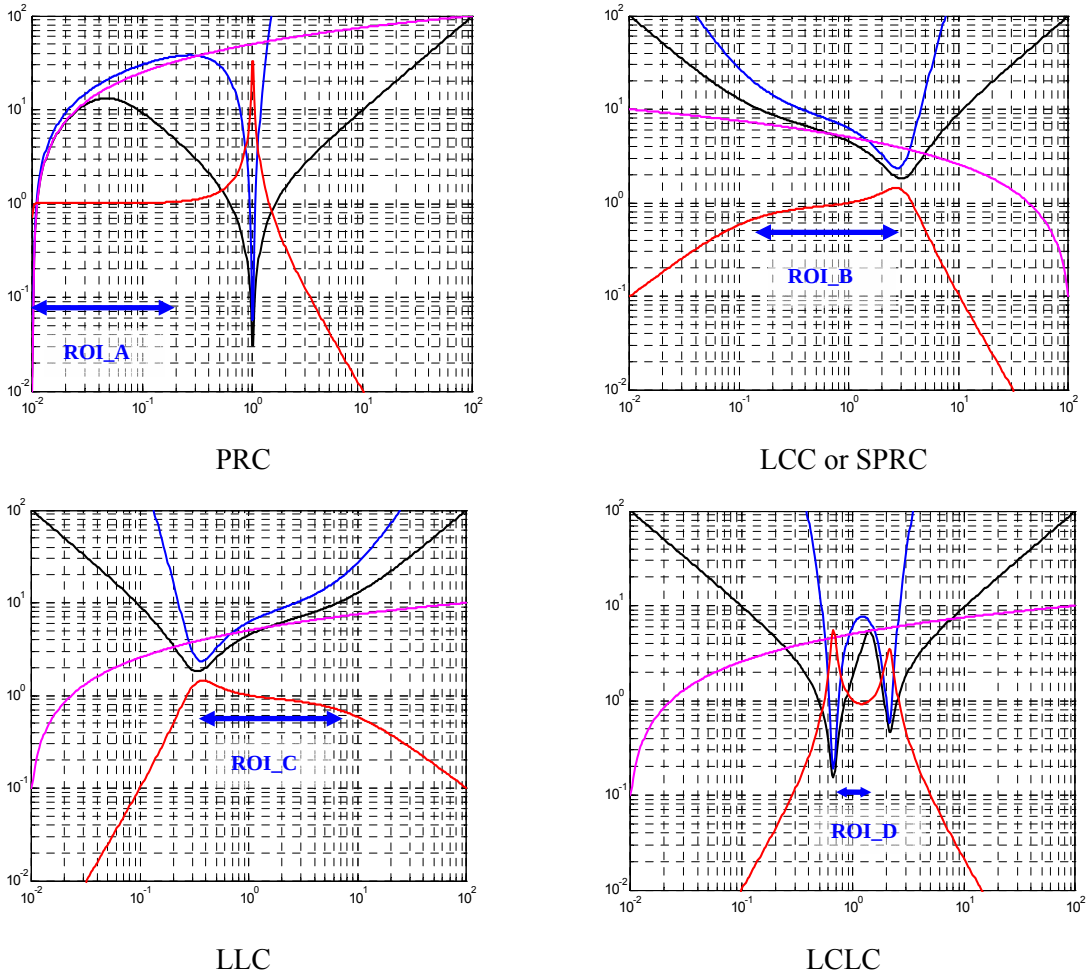

Figure 4. Normalized output voltage (red color), resonant tank impedance (black color) and converter input resistance (blue color) for the different resonant topologies considered

The analysis concludes that the LLC and the LCLC are the best choice as MPP trackers. Maybe the LLC a presents smaller variation on the output voltage than the LCLC, but the LCLC presents a larger variation on the input resistance and more sensibility to the frequency variations in this parameter. The design of the LCLC is more complex than that of the LLC due to the four resonant elements, but more versatile to be adapted to the applications requirements. For all these reasons the LCLC converter is chosen in this work.

Analysis of the LCLC Converter

Figure 5 shows the topology of the LCLC resonant converter and figure 6 its first harmonic model. The inverter stage (Full bridge) generate a square voltage waveform (v_s), and for the analysis only its first harmonic ($v_{s,1}$) is considered. This harmonic has a peak value of $4/\pi \cdot V_{gen}$. In the resonant tank a series load (Z_s) and a parallel load (Z_p) are considered. Finally, the load resistor (R_L), the output capacitor, the diodes rectifier and the transformer are modeled as an effective resistance (as is usual in the bibliography [4]) of value:

$$R_{Lef} = n^2 \frac{8}{\pi^2} R_L \qquad (2)$$

For the converter analysis the characteristic impedance ($Z_c^2=L/C$) and the natural frequency ($\omega_o^2=1/LC$) are considered as usually. The subscript s or p on these magnitudes denotes if they correspond to the series set or parallel set. The series and parallel resonant components present these impedance values:

$$Z_s(j\omega) = j\left(\omega L_s - \frac{1}{\omega C_s}\right) \qquad Z_p(j\omega) = \frac{j\omega L_p R_{Lef}}{j\omega L_p + R_{Lef}\left(1-\omega^2 L_p C_p\right)} \tag{3}$$

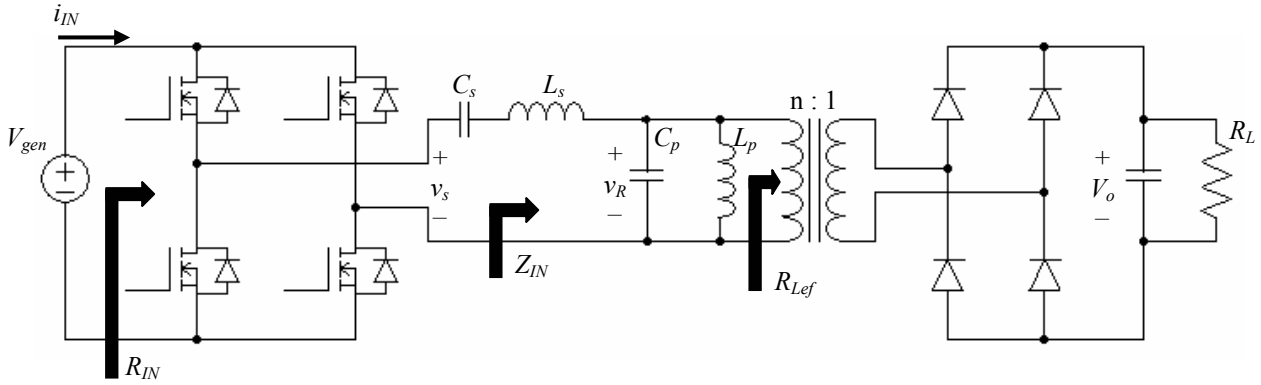

Figure 5. The LCLC converter

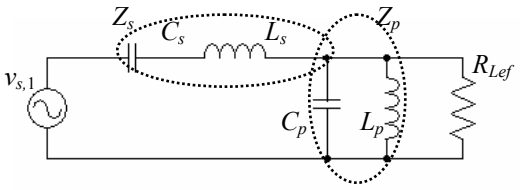

Figure 6. Sinusoidal model of the LCLC converter

The total impedance of the resonant tank (Z_{IN}) is the addition of Z_s and Z_p. Applying the changes presented in (4) in equations (3), the expression (5) is obtained.

$$k_L = \frac{L_p}{L_s} \qquad k_C = \frac{C_p}{C_s} \qquad \omega_{ns} = \frac{\omega}{\omega_{os}} \qquad IC = \frac{R_{Lef}}{Z_{cs}} \tag{4}$$

$$\frac{Z_{IN}(j\omega)}{Z_{cs}} = j\left(\omega_{ns} - \frac{1}{\omega_{ns}}\right) + \frac{jk_L\omega_{ns}}{jk_L\omega_{ns}\frac{1}{IC} + 1 - k_L k_C \omega_{ns}^2} \tag{5}$$

The transfer function between the first harmonic of the square wave form ($v_{s,1}$) and the voltage in the parallel load (v_R) is:

$$H(j\omega) = \frac{v_r}{v_{s,1}} = \frac{\dfrac{Z_p(j\omega)}{Z_{cs}}}{\dfrac{Z_s(j\omega)}{Z_{cs}} + \dfrac{Z_p(j\omega)}{Z_{cs}}} \tag{6}$$

The normalized output voltage is obtained considering continuous conduction mode in the transformer. The voltage v_r depends on the excitation $v_{s,1}$, left side of equation (7), and the output voltage V_o , right side of equation (7).

$$\frac{4}{\pi}V_{gen}\cdot\left|H(j\omega)\right| = v_r = \frac{4}{\pi}nV_o \tag{7}$$

From the relation obtained in (7), the normalized output voltage in the converter is (8).

$$n\frac{V_o}{V_{gen}} = \left|H(j\omega)\right| \tag{8}$$

The input resistance R_{IN} of the converter is obtained by means of equation (9), being i_{IN} the input current supplied by the input generator. This current depends on the voltage $v_{s,1}$ and the impedance of the resonant tank Z_{IN} . The normalized input resistance is presented in equation (10), being γ the angle of Z_{IN}. This angle determines the difference of phase between the waveforms of v_s and the current in the series resonant components.

$$R_{IN} = \frac{V_{gen}}{\frac{1}{T_s/2}\int_{t_i}^{t_f}\hat{i}_{IN}\sin(\omega t)dt} = \frac{V_{gen}}{\frac{1}{\pi}\frac{\frac{4}{\pi}V_{gen}}{|Z_{IN}|}\left[-\cos(\alpha)\right]_{\alpha_i=-\gamma}^{\alpha_f=\pi-\gamma}} \tag{9}$$

$$\frac{R_{IN}}{Z_{cs}} = \frac{\pi^2}{8}\frac{\frac{|Z_{IN}|}{Z_{cs}}}{\cos(\gamma)} \tag{10}$$

Simulation and experimental results

The selection of the converter components can be a tedious work due to the large quantity of magnitudes to choose: k_L, k_C, Z_{cs} and range of switching frequencies. The better set of components values will be those that minimize the error between the real R_{IN}, Z_{IN} and V_o with respect to the desired values. Table I presents the output current, voltage and power delivered of the PV module STP-165 (*Suntech*, monocrystalline silicon) employed on the experimental set-up. These values correspond to the average maximum extraction of energy of the panel at the location of Barcelona (Spain) in April. These values depend on the time of day and therefore of the irradiance on the panel. The output voltage for the most important solar times (from 9h to 18h) is close to 33,7 V. The output power varies from 45 W to 118W, and the input resistance in the converter must vary from 10Ω to 23Ω.

Table I: Information of the PV generator

	Current (A)	Voltage (V)	Power (W)	Input Resistance (Ω)
6 h	0,1	27,3	2,8	268,5
7 h	0,6	31,6	19,0	52,7
8 h	1,3	33,2	43,2	25,5
9 h	2,0	33,8	68,5	16,7
10 h	2,7	34,1	91,0	12,7
11 h	3,1	34,1	105,2	11,1
12 h	3,3	34,1	111,1	10,4
13 h	3,5	34,0	117,9	9,8
14 h	3,3	33,9	112,8	10,2
15 h	3,0	33,8	103,0	11,1
16 h	2,6	33,6	88,1	12,8
17 h	2,1	33,3	69,8	15,8
18 h	1,4	32,6	45,3	23,4
19 h	0,6	30,9	19,4	49,1
20 h	0,1	26,9	3,2	222,8

In order to find this set of components values, a genetic algorithm was programmed. The results from the iterations of the algorithm are: f_{os}=73kHz, Z_{cs}=18.6Ω, k_L=1.18, k_C= 0.45, f_s=[0.8 0.9]·f_{os}. With these constants, the resonant components are: C_s =117nF, L_s =40.6µH, C_p =53.1nF, L_p =47.7µF. Finally, in the experimental prototype the resonant components are L_s =44µH, L_p =47µH, C_s =100nF and C_p=50nF. The transfer turn ratio is n =0.56.

Figure 7 shows the input effective resistance (R_{IN}) of the converter at different switching frequencies (f_s). The values presented have been obtained testing the prototype, being a DC power supply the input element (not a PV module) and an active load. On the test, both the input voltage and the output voltage in the converter are constant values (30V and 40V, respectively), and the input and output current is measured at different switching frequencies. The results confirm that the behavior on R_{IN} variations is as expected on the analysis developed.

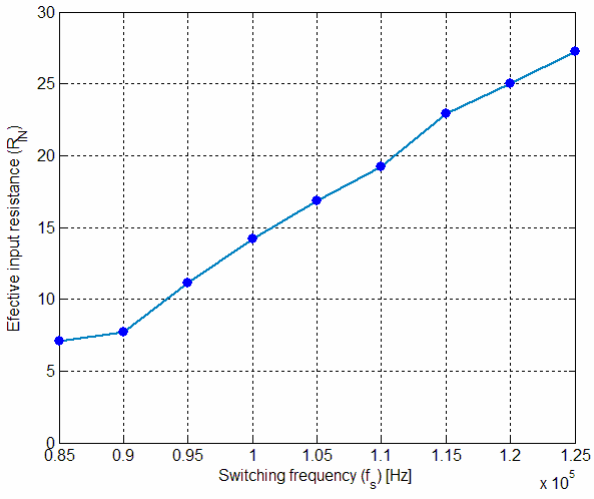

Fig. 7: R_{IN} [Ω] variations versus switching frequency [Hz] being V_o/V_{gen} a constant value

Table II presents experimental (input with a PV module) and simulations results obtained from the prototype and PSIM software at same conditions. The two cases presented correspond to different irradiation values, working the converter in the MPP. The values obtained in experimental results agree with the simulations. The first case corresponds to a switching frequency f_s=87.6 kHz, being the input resistance of the converter 12.1Ω. The second one corresponds to a switching frequency f_s=83.0 kHz, being the input resistance of the converter 7.6Ω.

Table II: Experimental and simulation results

			Experimental		Simulation		
f_s (kHz)	R_L	V_{gen} (V)	V_o (V)	I_{IN} (A)	V_o (V)	I_{IN} (A)	
87,6	33,0	31,4	47,2	2,60	50,0	2,51	(Figure 8 left)
83,0	16,5	28,6	35,7	3,73	41,3	3,70	(Figure 8 right)

Figure 8 shows the most significant waveforms obtained from simulation of the converter, based on the operating conditions and results presented in Table II. The difference between experimental values and simulations results is large in the output voltage, being small in the input current (I_{Ls}).

 ISBN: 9789075815009

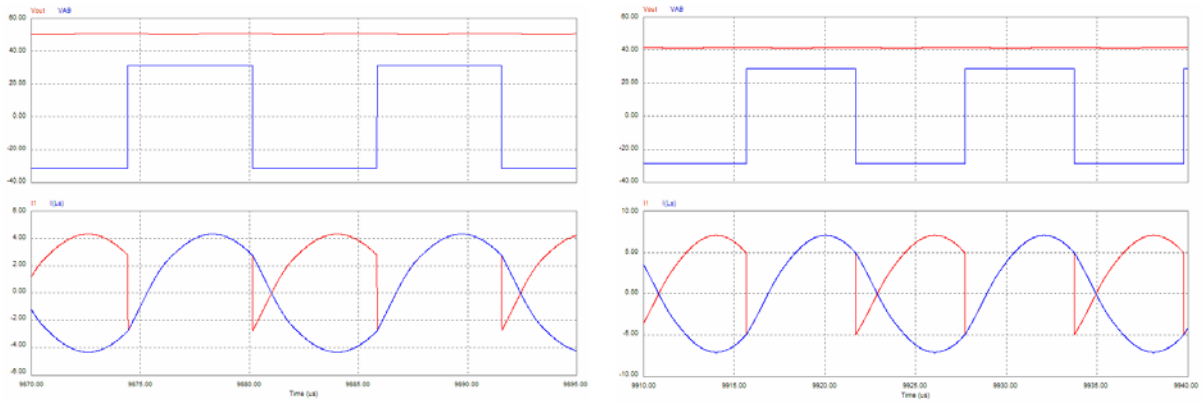

V_o : top figure in red, v_s: top figure in blue, i_{IN} : bottom figure in red, i_{Ls}: bottom figure in blue.

Fig. 8: Simulation results of the LCLC converter. On the left f_s=87.6 kHz. On the right f_s=83.0 kHz

Figure 9 shows the resonant current in the series inductance L_s on the left. It corresponds to a peak current value of 7.5 A. The output voltage of the inverter stage (v_s) is presented on the right.

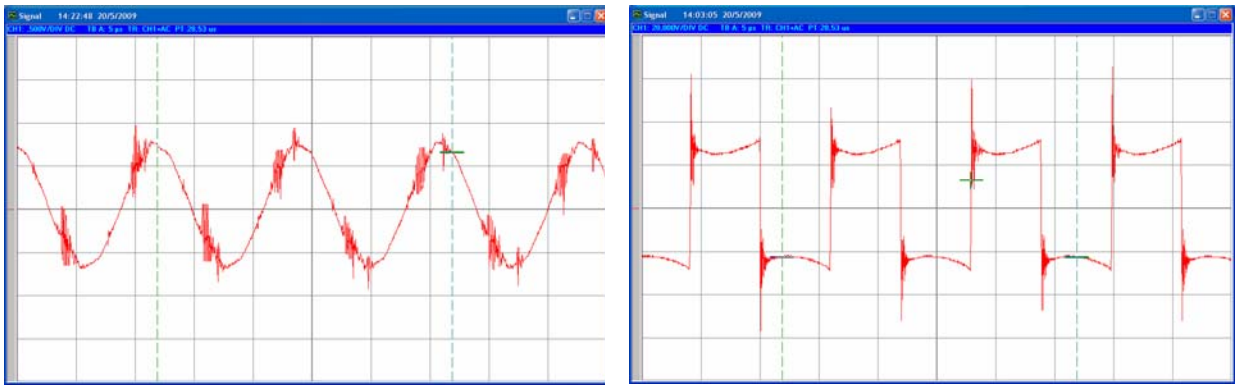

Fig. 9: Experimental results of the LCLC converter (i_{Ls} on the left and v_s on the right)

Figure 10 shows the voltage v_{DS} (blue color) and current I_D (red color) on a MOSFET on the left. The input voltage to the diode rectifier is presented on the right.

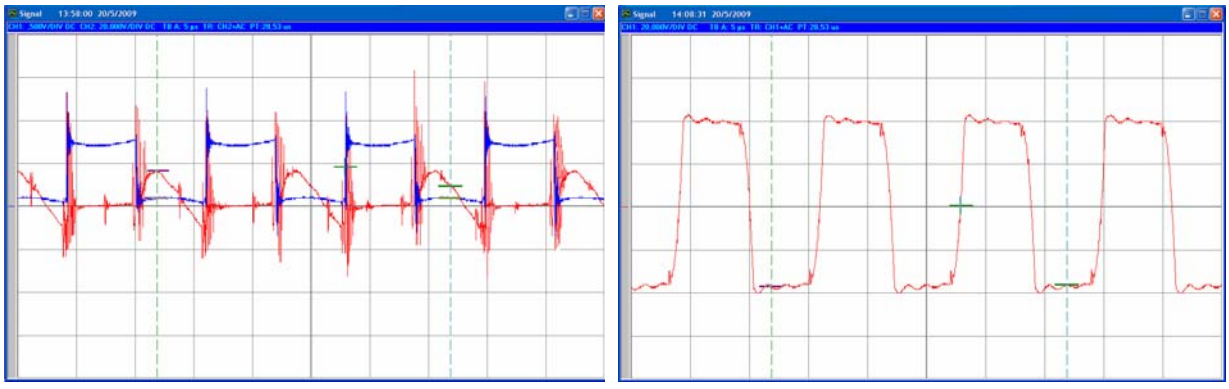

Fig. 10: Experimental results of the LCLC converter (v_{DS} and i_D on the left and v_{rec} on the right)

The results obtained conclude that the LCLC achieve the desired input resistance in the converter with variation of the switching frequency. The peak reactive current in the resonant components (i_{Ls}) is not a large value with respect to the average input current of the converter, as is desired in the study of the possible topologies. Finally, the output voltage varies with respect to the input power and is not a constant value as desired, but these variations are smaller than 16%.

Conclusions

A Maximum Power Point Tracker based on a LCLC resonant converter is presented. There are several resonant load topologies, but not all can be of interest to implement a MPP tracker in PV systems. Only the LLC and the LCLC can vary the input resistance of the converter keeping almost constant the output voltage. In this work the LCLC has been analyzed, and a prototype has been built. The simulation and experimental results agree with the analysis developed. The converter achieves the desired specifications according to the proposed test values in the PV system, being the choice of the resonant component values the most difficult task.

References

[1] Casaro, Marcio Mendes; Martins, Denizar Cruz. “Behavior Matching as fundamental feature to obtain a modified dual-stage inverter”. IEEE International Symposium on Industrial Electronics, 2008 (ISIE 2008). June 30 2008-July 2 2008 Page(s):2426 - 2431.

[2] Lamaison, R.M.; Bordonau, J.; Esquivel, A.; Peracaula, J. "Analysis and design of a resonant battery charger for photovoltaic systems". Proceedings of the IEEE International Symposium on Industrial Electronics, 1999 (ISIE '99). Volume 2, 12-16 July 1999, Page(s):463 - 468.

[3] Hohm, D.P. and Ropp, M.E. "Comparative study of maximum power point tracking algorithms using an experimental, programmable, maximum power point tracking test bed". Conference Record of the Twenty-Eighth IEEE Photovoltaic Specialists Conference, 2000 (28th PVSEC). On page(s): 1699-1702.

[4] Erickson, R.W.; Maksimovic, D. “Fundamentals of Power Electronics”, 2º Edition. Kluwer Academic Publishers 2001.

[5] Rossetto, L.; Spiazzi, G. "Series resonant converter with wide load range". The 1998 IEEE Industry Applications Conference (Thirty-Third IAS Annual Meeting, 12-15 Oct. 1998). Volume 2, Page(s):1326 – 1331.

[6] Alfonso Conesa, Robert Piqué and Enric Fossas. "The Serial Resonant Converter with Controlled Rectifier Stage". European Power Electronics Specialist Conference (EPE 2005, Dresden, Germany).